Supramolecular Materials: Self-Organized Nanostructures

S. I. Stupp,* V. LeBonheur, K. Walker, L. S. Li, K. E. Huggins, M. Keser, A. Amstutz

Miniaturized triblock copolymers have been found to self-assemble into nanostructures that are highly regular in size and shape. Mushroom-shaped supramolecular structures of about 200 kilodaltons form by crystallization of the chemically identical blocks and self-organize into films containing 100 or more layers stacked in a polar arrangement. The polar supramolecular material exhibits spontaneous second-harmonic generation from infrared to green photons and has an adhesive tape–like character with nonadhesive-hydrophobic and hydrophilic-sticky opposite surfaces. The films also have reasonable shear strength and adhere tenaciously to glass surfaces on one side only. The regular and finite size of the supramolecular units is believed to be mediated by repulsive forces among some of the segments in the triblock molecules. A large diversity of multifunctional materials could be formed from regular supramolecular units weighing hundreds of kilodaltons.

One of the great challenges for materials science is the creation of supramolecular materials in which the constituent units are highly regular molecular nanostructures. For organic materials, self-assembly of large oligomers into supramolecular polymers of 10^2 kD or more has the potential for creating such nanostructures. If necessary for the control of properties, chemical reactions internal to the units could transform them to shape-invariant covalent polymers, and external ones could interconnect them into stable morphologies. We believe that learning how to create large supramolecular units, and the elucidation of rules mediating their macroscopic organization into functional materials, will offer a fascinating prospect for technology.

Supramolecular chemistry has already demonstrated the possibility of assembling well-defined smaller structures, as pioneered by Lehn and co-workers (*1*). Whitesides and co-workers have also studied a number of systems with the objective of synthesizing well-defined nanoscale compounds with molar masses of a few kilodaltons (*2*). The self-assembly of other similar organic structures through hydrogen bonds has also been studied in the context of dendrimers (*3*), and polydisperse systems that form liquid crystals by hydrogen bonding have been studied by Frechet and co-workers (*4*). Our laboratory has reported on the combined use of self-assembly and chemical reaction in chiral monomers to generate two-dimensional (2D) polymers (*5*). We have also investigated the formation of nanostructures by self-assembly, using diblock polymer molecules termed "rodcoils," having a rigid rodlike segment covalently attached to a molecularly flexible coil-like segment (*6*). We found that rodcoil polymers can self-assemble into long striplike aggregates measuring 1 μm or more in length and a few nanometers in other dimensions. As the flexible segment of the rodcoil polymer increased in length relative to the rodlike segment, the molecules self-assembled into discrete disklike aggregates.

Our goal in this work has been to study strategies that could be used to create huge numbers of supramolecular units with similar size and shape. Such synthetic nanostructures, analogous to folded proteins in the definition of chemical sectors, shape, and topography, will be interesting building blocks for materials because they must pack in ways that fill space efficiently. For simple geometrical shapes such as flat objects, rods, and tubules, the 3D packing can be easily predicted. Flat objects such as 2D polymers are likely to stack and form layered structures (*5*), tubules and rods align uniaxially, and identically shaped and sized nanostructures such as the parallelepipeds are likely to tile into a wide variety of superlattices (Fig. 1).

One could envision a variety of functional materials synthesized with supramolecular nanostructures. One possibility is micro- or macroscopic structures made up of stacked plates with surface properties that directly reflect the chemical exterior of flat nanostructures. Another example would be cables or microfibers formed by aligned nanotubes that could select and direct molecules or ions in space. It is also possible to envision macroscopic objects or lithographically fabricated domains made up of superlattices formed by nanostructures with sensing features. Such features could include cavities or protrusions that present to an external environment large arrays of binding sites for small or large molecules. Alternatively, similar superlattices may function as membranes because the packing of nanostructures (depending on their shape) could create free volume that is available for the selective flow of liquids or gases. Macroscopic organization of such nanostructures could help us learn what is needed to develop highly functional materials that behave as devices and are created on demand without the use of complex hardware. It would also provide us with abiotic systems with which we could learn about self-assembly on the length scales of biological systems. The work reported here describes the self-assembly of mushroom-shaped nanostructures built from small-molecule precursors with chemical sequences inspired by

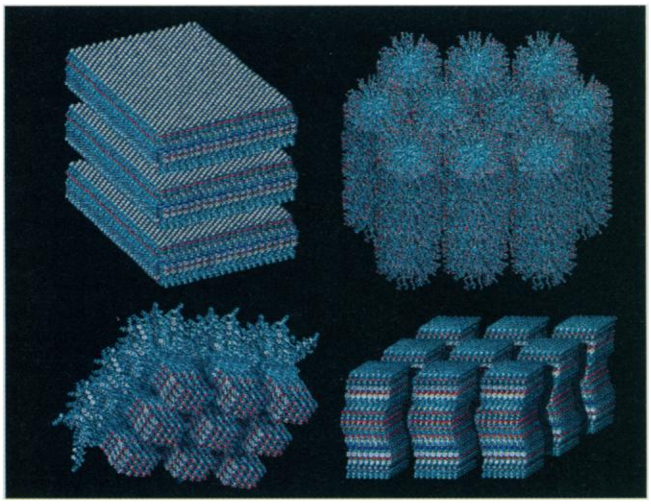

Fig. 1. Supramolecular nanostructures with well-defined shapes and sizes are likely to pack into predictable structures. Plates are likely to stack with a common stacking direction, and tube- or rodlike nanostructures would tend to align uniaxially. Regularly sized and shaped nanostructures may tile into superlattices of varying geometries and symmetries.

The authors are in the Department of Materials Science and Engineering, Department of Chemistry, Beckman Institute for Advanced Science and Technology, Materials Research Laboratory, University of Illinois at Urbana-Champaign, Urbana 61801, IL, USA.

*To whom correspondence should be addressed.

block copolymer chemistry.

Synthesis. We synthesized molecules with the following structure, which can be described as miniaturized triblock polymers.

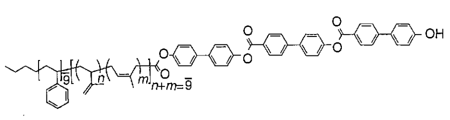

1

The synthesis starts with the reaction known as living anionic polymerization, studied extensively by Szwarc (*7*) (using in this case styrene monomer initiated by *n*-butyl lithium). However, the amount of monomer supplied is only sufficient to create a miniature styrene chain with an average degree of polymerization of 9. A second block with a similar average degree of polymerization grows when isoprene is added, acting as an electrophile to the living anions in the reaction medium (*8*). In a third step, CO_2 quenches the isoprenic living anion and installs carboxyl end groups at the end of the miniature diblock copolymers (*9*). This carboxyl group can then be used as a junction point to attach the third block by esterification reactions. As shown in Scheme 1 (*10*), the third block in **1** is a rigid chemical sequence built by the esterification of **2** and **3**, followed by deprotection at the phenolic terminus and a second esterification of compounds **4** and **5** [PhH, benzene; THF, tetrahydrofuran; DPTS, 4-(*N*-*N*-dimethylamino) pyridinium-4-toluenesulfonic acid; DIPC, diisopropyl carbodiimide; $CHCl_3$, chloroform; RT, room temperature]. The final triblock structure (**1**) is obtained after a second deprotection of the phenolic terminus. This triblock structure has two aperiodic blocks that are chemically diverse in the system and one rodlike block that is identical in all molecules. One terminus of the triblock is a hydrophobic methyl group (from the *n*-butyl lithium initiator), and the opposite terminus is hydrophilic, consisting of a phenolic group.

These triblock molecules have a rodcoil architecture, because a stiff rodlike segment is covalently connected to a more torsionally flexible diblock segment that in solution adopts coil-like conformations. The polydispersity of the triblock molecules (ratio of the weight-averaged to number-averaged molecular weights) measured by gel permeation chromotography with the use of polystyrene standards ranges from 1.06 to 1.1. Numerous chemical sequences are possible for the coil diblock, generating great structural diversity in the system. The styrene block is atactic and is thus a random sequence of meso and racemic diads; the isoprene segment has mostly repeats from 1,4 and 3,4 addition (based on nuclear magnetic resonance data) but can also have a trace of 1,2 units. Although both blocks are nonamers on average, the diblock sequences should have a distribution of molar mass comparable to a Poisson distribution. On the basis of field-desorption ionization mass spectrometry of short styrene segments, the distribution may be slightly narrower than a Poisson one. The molar mass distribution contributes further to the structural diversity in chemical sequence among the triblock molecules of the system. In contrast, the rod segment is analogous to a chemical compound, and it is therefore the common structural element shared by all molecules in the system.

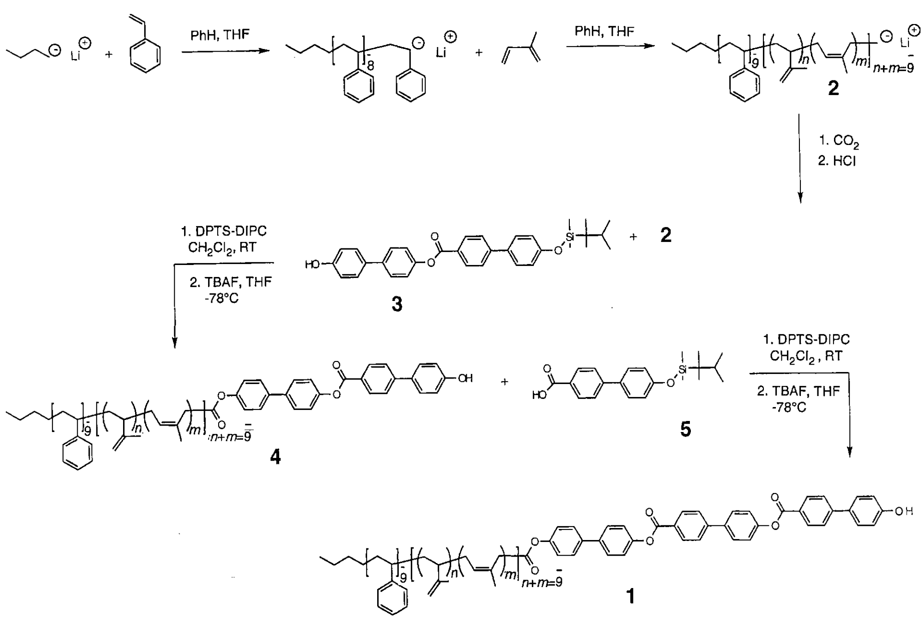

Scheme 1

Supramolecular and thin film structure. When thin films of the triblock molecules were cast from dilute chloroform solutions (1 mg/ml), nearly identical nanosized aggregates formed, as revealed by the transmission electron microscope (TEM) micrograph in Fig. 2 (no staining compounds were used); Fig. 2 also shows the wide-angle and small-angle electron diffraction (ED) patterns corresponding to the image, indicating that the observed nanosized aggregates (dark spots) are crystalline. We obtained the image using a large objective aperture (40 μm), and the image was properly underfocused to enhance contrast. Under the conditions used, the image in Fig. 2 contains both diffraction and phase contrast. Because the only segment that could organize into a crystalline lattice is the rodlike segment, the dark regions observed probably consist of ordered clusters of the rigid biphenyl ester blocks. The wide-angle ED pattern reveals an a*b* reciprocal lattice plane, indicating that rod segments are oriented normal to the plane of the micrograph. All of the dark spots are of similar shape and size, which indicates that these aggregates must contain about the same number of molecules. The similarity in shape and size is fingerprinted by self-organization of the aggregates into a superlattice with periodicities of 70 and 66 Å. The image and small-angle ED pattern in Fig. 2 show the planar superlattice to be oblique with a characteristic angle of 110°. If the superlattice were monoclinic in three dimensions, then the aggregates shown in the image would be positioned at the lattice points of an (001) plane.

Crystallization of the identical rodlike segments in the miniature triblock polymer must exclude the chemically diverse oligostyryl and oligoisoprene blocks. In our view, the chemical aperiodicity and diversity of these two segments in the triblock population of molecules is an extremely important factor in the formation of supramolecular units observed here. These two segments frustrate the global ordering of the system, thus preventing the formation of a 3D crystal as expected when all molecules are identical. Thus, the disruption of chemical regularity in two of the blocks in each triblock molecule predisposes the system to form finite aggregates. The oligoisoprene segment is conformationally flexible, given that polyisoprene is a rubber at room temperature, and also has a small cross-sectional area relative to the styrene segment. The isoprene blocks therefore serve as a structural buffer that can stretch and pack to accommodate the density of the crystallized rodlike segments.

The biphenyl ester segments have an extremely high tendency to aggregate and order through π-π overlaps. This is fairly evident in the insolubility of a compound containing only the rodlike segment of the triblock structure. Also, polymers with similar structures in their chemical repeats have extremely high melting points if they fuse at all before reaching the regime of chemical decomposition. Because oligostyrene segments have a fairly large cross section, they will encounter strong hard-core repulsive forces when trying to accommodate the nanocrystal's density. These repulsive forces could balance the favorable association of aromatic blocks and prevent the infinite aggregation of triblock molecules. This effect is illustrated by a computer model in which an empirical force-field calculation is used on a small cluster of seven triblock molecules arranged parallel to each other (*11*). Figure 3 shows the cluster of triblock molecules before complete energy minimization, color coded for energy and pointing to the larger cross section styrene segments as a site of high repulsive energy. In the fully relaxed cluster (right side of Fig. 3), the growth of an incipient mushroom-shaped nanostructure is evident. Calculations based on the use of the same model (*11*) indicate that forces among densely packed molecular segments remain attractive for rod blocks and repulsive for styrene-isoprene blocks in either parallel or antiparallel arrangements. Interestingly, however, the parallel arrangement of blocks leading to a mushroom-like aggregate is the most favorable, according to the calculated packing energies. We refer to parallel and antiparallel arrangement of blocks as ferro and antiferro clusters, respectively, and the energies of all four possibilities are given in Fig. 4. On the basis of the packing energies, one would conclude that fully interdigitated rod and coil segments would not be a favorable molecular arrangement in the units observed. However, the supramolecular units may consist of mushroom-shaped aggregates with molecules arranged in parallel or of dumbbell-shaped ones in which only rod segments interdigitate in antiparallel fashion.

A balance of attractive and repulsive forces among blocks could mediate the formation of supramolecular units. However, a different mechanism based on entropic effects could lead to their formation. In addition to the usual entropic penalties linked to molecular aggregation (translational), an additional entropic loss associated with this system could be linked to the required stretching of the flexible coil segments in order to accommodate rod-rod interactions. Finite aggregation into nanostructures reduces this penalty because it allows coils to splay at the periphery of the supramolecular unit (*6*). Thus, this mechanism for nanostructure formation could be important even in systems of identical molecules with very large, molecularly flexible segments. In the triblock molecules studied here, the coil diblock segments are not very long or extremely flexible. Thus, the balance of attractive and repulsive forces among blocks may be more important. Finite aggregation may also prevent the entropically unfavorable vitrification of packed coil segments exposed to repulsive interactions.

Fourier-transform infrared spectroscopy indicates that annealing of the films at 250°C for 2 hours leads to cross-linking of the triblock molecules by reaction among isoprene segments, consuming about 40% of their double bonds. This reaction, which has a well-defined exothermic signature in differential scanning calorimetry scans at a rate of 20°C/min (with an onset temperature of 300°C), does not appear to form a 3D gel. Once cross-linking occurs, the samples remain thermoplastic and a birefringent melt is observed at 250°C (*12*). Isotropization of the birefringent fluid is never observed before chemical decomposition above 400°C. After cross-linking, the crystalline order of rod segments in the self-assembled aggregates improves as revealed by ED. We do not know at this time if the reaction is confined within the discrete supramolecular units, transforming them to covalent polymers. However, a thermosetting 3D network does not form as a result of cross-linking among isoprene segments.

Solution-cast films coated with C on one side and placed on Au grids were embedded in epoxy for ultramicrotomy. These films were ~1 μm thick and, before the embedding procedure, had been annealed at 250°C for 2 hours and also had been exposed to a stain of OsO_4 vapors for 15 hours (*13*). Sections from films ~1 cm^2 in area and ~1 μm thick were made up of many layers, all oriented with a common layer normal. The characteristic period of the layers with a common stacking direction

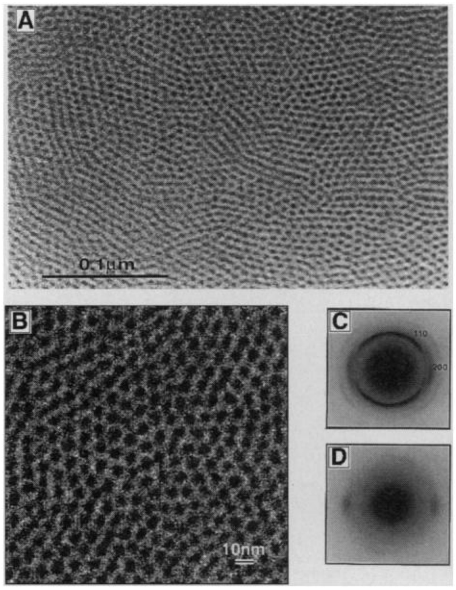

Fig. 2. (**A**) Transmission electron micrograph at low magnification [with a high-magnification image shown in (**B**)] of a film formed by the triblock molecules, revealing regularly sized and shaped aggregates that self-organize into superlattice domains. Wide-angle (**C**) and small-angle (**D**) ED patterns are also shown.

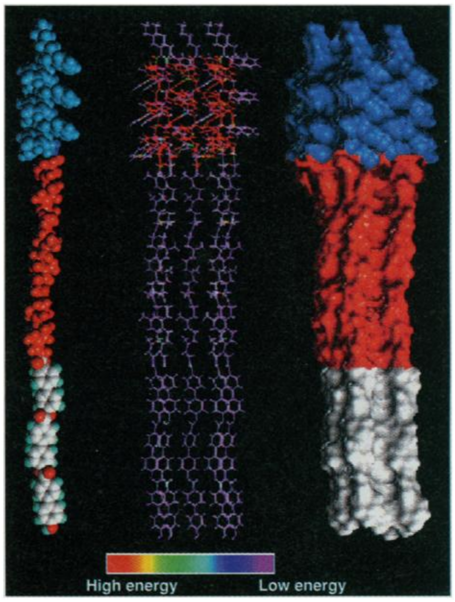

Fig. 3. Molecular graphics of the triblock self-assembling molecule (left); cluster of triblock molecules before complete energy minimization, color-coded for energy in different sectors of the cluster (middle); a relaxed cluster revealing the incipient mushroom architecture (right).

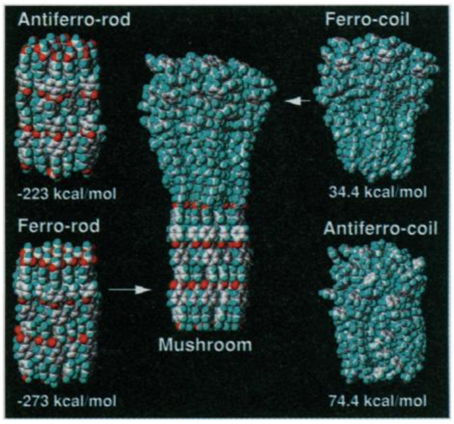

Fig. 4. Two different molecular clusters composed of 13 coil-like diblock segments (right) arranged parallel to each other (ferro cluster) or antiparallel to each other (antiferro cluster). At left the same two types of clusters are shown for the rod segments of triblock molecules. The calculated energies associated with these four clusters suggest that a mushroom cluster of triblock molecules would be favored by the system.

was ~70 Å, consisting of one dark and one light band with thicknesses of 30 and 40 Å, respectively. A TEM micrograph of one of the ultramicrotomed sections at two different magnifications is shown in Fig. 5 together with a Fourier-filtered image (*14*) revealing very clearly the periodicity and orientation of the layers. We obtained this Fourier-filtered image using only the meridional intensity in the Fourier transform to highlight the layered nature of the self-organized film.

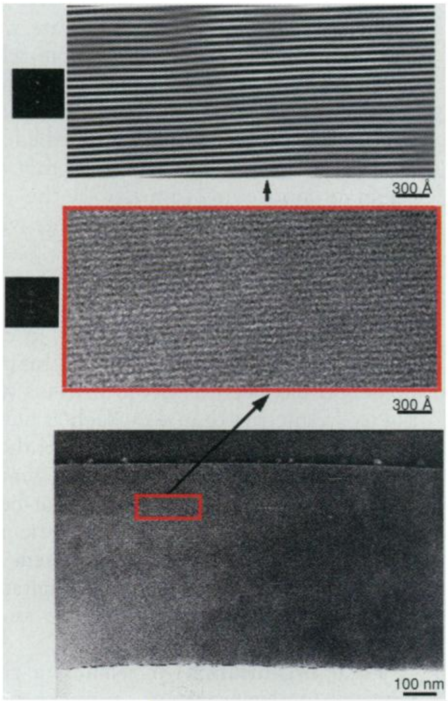

Fig. 5. Transmission electron micrograph of an ultramicrotomed section obtained from a film 1 μm thick by use of a diamond knife (bottom). A section of the image viewed under higher magnification (middle). Its Fourier-filtered image was obtained only with meridional intensity in the Fourier transform in order to highlight the lamellar periodicity of the film (top).

The electron micrograph of the ultramicrotomed films reveals information on how the nanostructures might be stacked to form the macroscopic films. We interpret the dark and light bands to be regions containing the crystalline rods and the amorphous coil segments, respectively. This interpretation is based on two facts. (i) The thickness of dark bands is roughly equivalent to the length of one extended rod segment, and (ii) a rather strong diffraction contrast results from the crystallization of rod blocks alone, as demonstrated by the micrographs of an unstained sample in Fig. 2. The thicker light band, on the other hand, has a thickness corresponding to a single nonextended styrene-isoprene segment (the fully extended length of an average segment would be ~60 Å). The OsO_4 stain did not seem to provide any additional contrast, and this may be due to cross-linking among isoprene units during annealing.

Additional evidence for a characteristic periodicity in films equivalent to one triblock molecule was obtained by electron microscopy of Pt-shadowed samples. These shadowed samples were imaged at their edges where the films were thinnest. All the distinct steps or terraces observed in the films had dimensions definitely under 100 Å, thus suggesting that the nanostructures self-organize as monolayers and not as bilayers. The observed period of ~70 Å rules out the dumbbell-shaped supramolecular structure in which only rods are interdigitated, even though this would create more volume for the flexible segments to explore conformational space. However, one must still consider the possibility that interdigitation of both rods and coils occurs in these supramolecular units. However, as mentioned before, the interdigitation of both rod and diblock coil segments in antiferro clusters may not be favorable given the large cross section of styrene blocks (see Fig. 4). If diblock coils cannot interdigitate, the interpretation of TEM images must be that molecules are assembled into nanostructures that are one molecule thick with nanophase separation of all three blocks. Furthermore, in order for this type of aggregate to generate an image with layers of alternating light and dark bands, the nanostructures must be stacked in polar fashion and not antiparallel to each other within the layers.

On the basis of the wide-angle diffraction pattern of Fig. 2, the rodlike segments are packed into an orthorhombic unit cell with lattice parameters equal to 5.4 and 8.2 Å. Using these unit cell parameters as well as the cross section and thickness of nanostructures observed in TEM images, we estimate that there are approximately 100 molecules in each nanostructure. The supramolecular units would then have a molar mass of approximately 200 kD. Also, the nature of the superlattice (oblique with two characteristic dimensions as opposed to hexagonal or cubic) suggests that the supramolecular aggregates have cross sections that are more rectangular than circular in shape. On the basis of data presented so far, we are led to the heuristic model of the nanostructure shown in Fig. 6 that envisions it as a mushroomlike aggregate of about 100 triblock molecules. In this mushroom aggregate, the chemically aperiodic and structurally diverse coil segments are excluded from the crystalline sector formed by identical rod segments. If we regard the aggregate as a shape-invariant supramolecular polymer, the system would be one with a fairly narrow distribution of size and shape.

The model in Fig. 7 envisions the films (1 μm thick and 1 cm^2 in area) prepared in our laboratory as the layered assembly of trillions of mushroom-shaped nanostructures, arranged with polar order in the lay-

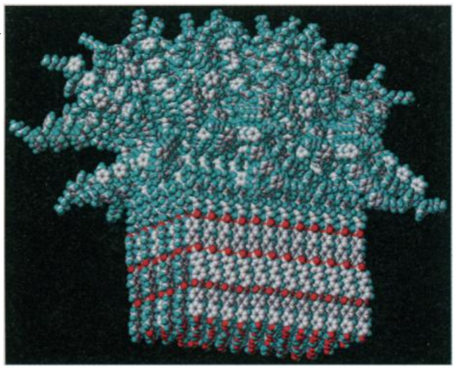

Fig. 6. Molecular model of the supramolecular unit composed of 100 triblock molecules and a molar mass of about 200 kD. Rod segment packing in the mushroom stem is based on electron diffraction data and its rectangular shape on the observation of an oblique superlattice of nanostructures.

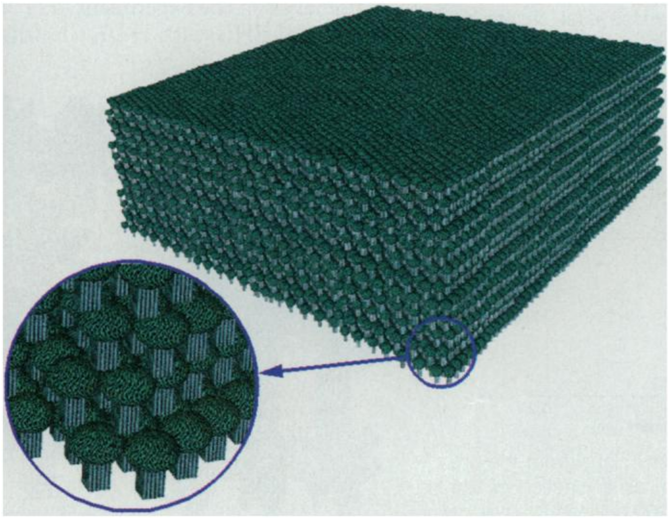

Fig. 7. Schematic representation of how mushroom nanostructures formed by triblock molecules might organize to form the macroscopic film. The nanostructures are stacked with polar order, always producing a surface of caps and an opposite surface of stems. The 3D details of nanostructure stacking are not known, but within one layer we have observed an oblique arrangement of the aggregates.

ered stacking. The TEM images of single layers of nanostructures revealed the presence of oblique superlattice domains within one layer. We do not know, however, if the mushrooms organize with 3D order or if the stacking is uncorrelated through the layers. In other more symmetric molecular nanostructures studied in our laboratory, 3D order was observed across several layers (*15*), and so this possibility cannot be ruled out at this time. Even if a stacking order were to exist, we would expect a given concentration of stacking faults and point defects, as is common in most materials.

Surface properties. We measured contact angles made by water droplets on the surfaces of films cast from chloroform solutions on a water surface, picked up on glass slides, and dried thoroughly under Ar. Top surfaces of these films (air side) were always highly hydrophobic, and contact angles for water of approximately 98° ± 1° were observed. When we inverted the films by means of adhesive tape before complete drying and then dried them thoroughly under Ar, the contact angles observed for water were always lower (approximately 27° ± 2°), indicating the formation of a more hydrophilic surface. The contrasting hydrophobic-hydrophilic character on opposite surfaces of these films was always observed even without any long annealing period after solvent evaporation. In contrast, long annealing periods (hours or days) are often required to observe contrasting surface properties in films of block copolymers that may contain hydrophobic backbones and hydrophilic end groups after being cast on polar surfaces (*16*). The observed surface behavior of films would be consistent but does not prove the formation of polar films by self-organization of the nanostructures. Water droplets on opposite surfaces of the supramolecular films are shown in Fig. 8.

Adhesion and mechanical properties. Supramolecular films cast on glass and thermally cross-linked adhere tenaciously to the substrate. This observed property could arise partly from hydrogen bonding between the substrate and the phenolic groups of rod segments. Aqueous hydrofluoric acid (HF) dissolves glass, and dilute solutions are routinely used to lift organic films cast on glass. We found that films could not be lifted from glass surfaces even at HF concentrations of 6.7 M, which visibly etch the glass, producing cracks and pits throughout its surface. In contrast, poly(vinyl phenol) films whose side chains of repeats are identical to the termini of rod segments in the supramolecular units are readily removed in a few minutes. Finally, two films fused between glass surfaces exhibited a shear strength equal to 1.22 MPa, at least twice that observed for a film of poly(vinyl phenol) of comparable thickness (0.53 MPa). The layered supramolecular film, without the benefit of extensive chain entanglements, exhibits a higher adhesive strength than does poly(vinyl phenol).

Nonlinear optics. A polar film envisioned in the schematic of Fig. 7 should not have a center of inversion and could therefore exhibit dipolar second-order nonlinear optical activity without the need for electrical poling. We measured and averaged the second harmonic generation (SHG) from films cast from solution on glass substrates and discovered that frequency doubling of an infrared laser beam at 1064 nm was indeed observed well above any possible noise levels in the experiment (*17*). The correlation of SHG with mean film thickness (measured by profilometry) is indicative of bulk polar structure in the macroscopic supramolecular film, as opposed to just broken symmetry at its surfaces (Fig. 9). Measurements taken with *p*-polarized light as the sample was rotated at 5° intervals about an axis in the plane of the film revealed a significant increase in SHG with rotation (the plane of the sample was tilted at an obtuse angle relative to the beam direction). Thus, the conjugated rod segments normal to the glass substrate must contribute to the signal. Furthermore, when the incident beam had *s*-polarization, essentially no signal was observed. The SHG signals were observed in both annealed and unannealed films, an indication that the origin of noncentrosymmetry is the self-organization of supramolecular units when films are cast from solution. One has to consider the possibility that the observed signal was the result of quadrupolar SHG, which has been observed recently in centrosymmetric films (*18*). However, this phenomenon has been observed in films with higher symmetries than ours, such as phthalocyanine films or C_{60} films. The phthalocyanine films investigated had D_{4h} symmetry and were prepared by molecular-beam epitaxy techniques. Because of steric factors, we do not believe that our system can have complete molecular interdigitation and the necessary symmetries for strong quadrupolar effects.

Polar organization. It remains a challenge to understand the origin of polar organization in the supramolecular material studied. Polar order is an extremely useful source of functionality in materials but is uncommon in nature. Polar structures are linked to properties of materials such as piezoelectricity, pyroelectricity, second-order nonlinear optical susceptibility, and ferroelectricity. Ideal polar order achieved with layered nanostructures also offers a strategy for creating films much thicker than a monolayer that would still have two chemically distinct

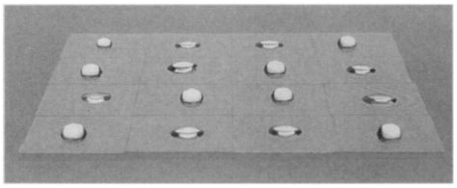

Fig. 8. Water droplets on the surfaces of 16 different supramolecular films placed on glass substrates in different orientations after casting on water. The receding contact angles of water indicate which surface of the polar film is exposed to air—the one with hydrophilic or hydrophobic sectors of the supramolecular units.

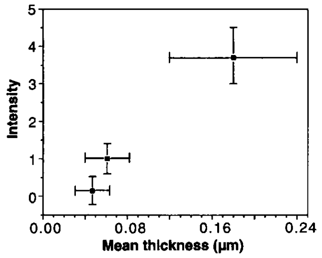

Fig. 9. Intensity of the SHG signal from the unpoled supramolecular film as a function of film thickness (average of 30,000 pulses).

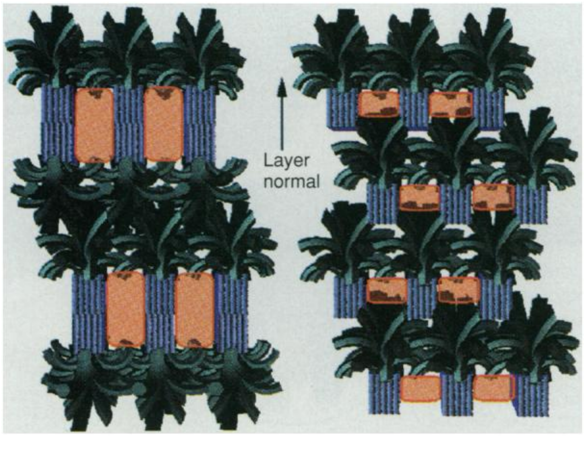

Fig. 10. Schematic representation depicting the smaller and more easily filled pores in monolayer stacking of nanostructures compared to pores formed in bilayer stacking. In bilayer stacking of these nanostructures, displacements parallel or perpendicular to the layer normal are not efficient at filling volume otherwise occupied by solvent (orange regions).

surfaces regardless of thickness, surface roughness, or erosion of molecular layers. Polar stacking of nanostructures in macroscopic supramolecular films could be related to efficient space filling by mushroom-shaped aggregates of molecules. We believe that minimization of free volume in these films is important because solvent (chloroform) is tenaciously retained even after films are heated to temperatures more than 100°C higher than the solvent's boiling point of 61°C (*19*). Chloroform is known to hydrogen-bond with carbonyl groups (*20, 21*) and thus could also bond with phenolic and ester bonds in rod segments. At an entropic cost, the solvent could fill space not occupied by the nanostructures, thus avoiding the presence of free volume. If solvent molecules interact strongly with rod termini, the contact energies between mushroom stems and caps would be minimized because bound solvent disguises their hydrophilic nature. Bilayer stacking could certainly create larger pores, which may be more difficult to fill with molecularly flexible segments by x, y, z translations of the nanostructures (Fig. 10), whereas polar monolayer stacking of the supramolecular units in three dimensions may fill volume more effectively by such translations. The caps of the mushroom nanostructures should be more deformable than the rod stems and therefore have the flexibility to fill space more efficiently. In the case of bilayer stacks, displacements parallel to the layer normal may not be effective at filling space. Thus, macroscopic objects composed of supramolecular bilayers may require for stability the entrapment of larger amounts of solvent in order to avoid free volume.

Our findings should encourage the search for multifunctional materials in solids composed of one or several types of supramolecular units with regular shape, surface chemistry, and dimension. Our discovery challenges the search for structurally diverse systems of simple molecules that can find energy minima in regular nanostructures defined by chemical sectors, topographical features, and global shape. Because of the potential for function integration, such supramolecular materials could affect the technologies of sensors, biomaterials, cell substrates, waveguides, membranes, materials coupling in composite structures, solid lubricants, and catalysts, among others.

REFERENCES AND NOTES

1. J.-M. Lehn, *Supramolecular Chemistry* (VCH Press, New York, 1995).
2. G. M. Whitesides, J. P. Mathias, C. T. Seto, *Science* **254**, 1312 (1991); C. T. Seto, J. P. Mathias, G. M. Whitesides, *J. Am. Chem. Soc.* **115**, 1321 (1993); J. P. Mathias, E. E. Simanek, G. M. Whitesides, *ibid.* **116**, 4326 (1994).
3. S. C. Zimmerman, F. Zeng, D. E. C. Reichert, S. V. Kolotuchin, *Science* **271**, 1095 (1996).
4. T. Kato and J. M. J. Frechet, *J. Am. Chem. Soc.* **111**, 8533 (1989); U. Kumar, T. Kato, J. M. J. Frechet, *ibid.* **114**, 6630 (1992).
5. S. I. Stupp, S. Son, H. C. Lin, L. S. Li, *Science* **259**, 59 (1993); S. I. Stupp *et al.*, *J. Am. Chem. Soc.* **117**, 5212 (1995).
6. L. H. Radzilowski and S. I. Stupp, *Macromolecules* **27**, 7747 (1994); L. H. Radzilowski, B. O. Carragher, S. I. Stupp, *Macromolecules*, in press.
7. M. Szwarc, *Carbanion, Living Polymers, and Electron Transfer Processes* (Wiley-Interscience, New York, 1968).
8. Benzene (90% by volume) and THF (10% by volume) were used as the polymerization solvents. THF was added to break up the aggregates that *n*-butyl lithium forms in benzene [M. Morton, *Anionic Polymerization: Principles and Practice* (Academic Press, New York, 1983)], thus increasing the rate of styrene oligomerization. We carried out the reaction at RT, using standard Schlenk line techniques with a freeze-pump-thaw procedure of solvents before initiation.
9. P. J. Manson, *Polym. Sci. Polym. Chem. Ed.* **18**, 1945 (1980); R. P. Quirk and W. C. Chen, *Makromol. Chem.* **22**, 85 (1989).
10. The esterifications in **1** are carried out under mild conditions developed by J. S. Moore and S. I. Stupp [*Macromolecules* **23**, 65 (1990)]. The reaction uses DIPC and DPTS.
11. The rod segments in this computer model have extended conformations, without kinks or bends along their length. We applied to the rod segments a genetic algorithm developed in our group for conformational energy minimization (M. Keser and S. I. Stupp, in preparation) and found that virtually all of the low-energy conformations found for these segments were fully extended. In order to calculate cluster energies, our program loads copies of a molecule into SYBYL and creates a very dense cluster. This cluster is then allowed to relax by means of the Tripos force field with conjugate gradient minimization, generating as output the cluster's energy. SIMPLEX minimization is first used for a few steps, and this often requires fixing awkward structures such as back-folded CH_2 units, hydrogen-pierced rings, and fused rings.
12. Before cross-linking, triblock molecules (**1**) form a birefringent solid at RT, which melts into a liquid crystal at about 130°C and undergoes isotropization at 262°C.
13. We used OsO_4 as a standard staining procedure for the remaining double bonds in isoprene segments in order to improve contrast in electron microscopy. After staining, the Au-organic-C sandwich was microtomed with a diamond knife into sections 50 to 100 nm thick. Gold was necessary for this procedure because of its softness. Moreover, the flanking of the organic film by Au and C on opposite surfaces offered an excellent tracer that could be used to find the film under the electron beam. Also, ultramicrotoming of the thin films is possible only after the cross-linking reaction, which increases the mechanical integrity of the film. We also find that, after cross-linking, atomic force microscopy tips do not mechanically damage the film's surface.
14. The image-processing technique known as fast Fourier transform enhances the signal-to-noise ratio in TEM images by removing the coefficients of the Fourier transform at spatial frequencies that do not correspond to the periodic structure of a specimen [D. L. Misell, in *Practical Methods in Electron Microscopy*, A. M. Glauert, Ed. (North-Holland, New York, 1978), vol. 7; A. Rosenfeld and A. C. Kak, *Digital Picture Processing* (Academic Press, New York, ed. 2, 1982), vol. 1; J. C. Russ, *The Image Processing Handbook*, (CRC Press, Boca Raton, FL, ed. 2, 1995)]. We filtered coefficients of the transform corresponding to structural detail from those corresponding to noise by multiplying the power spectrum by a "mask" having a value of unity near the coefficients of interest and zero elsewhere (the power spectrum is obtained from the fast Fourier transform of the digitized image and is analogous to an optical diffraction pattern).
15. L. H. Radzilowski, B. O. Carragher, S. I. Stupp, *Macromolecules*, in press.
16. J. F. Elman, B. D. Johs, T. E. Long, J. T. Koberstein, *ibid.* **27**, 5341 (1994).
17. Samples were mounted on a rotation-translation stage, and the 1064-nm fundamental was tightly focused on the center of the sample, yielding a peak intensity of 30 MW/cm^2. The 1064-nm fundamental was produced by a Molectron MY34-20 Q-switched Nd:yttrium-aluminum-garnet laser with a 20-ns pulse width operating at a 20-Hz repetition rate. The second harmonic at 532 nm was separated from the fundamental by means of a series of green pass filters and an Instruments SA, Inc. DH-10 double monochromator. The light was collected in a Hamamatsu R1477 photomultiplier tube, and the signal was sent out to a digital data-acquisition system and an oscilloscope. All data were corrected for transmission of fundamental and absorption of the second harmonic.
18. K. Kumagi, G. Mizutani, H. Tsukioka, T. Yamauchi, S. Ushioda, *Phys. Rev. B* **48**, 14488 (1993); D. Wilk, D. Johannsmann, C. Stanners, Y. R. Shen, *ibid.* **51**, 10057 (1995); H. Hoshi, T. Yamada, K. Ishikawa, H. Takeoze, A. Fukuda, *ibid.* **52**, 12335 (1995); *ibid.* **53**, 12663 (1996).
19. The presence of chloroform in cast films was established by infrared bands at 758, 1215, and 3025 cm^{-1}.
20. S. Wu, *Polymer Interface and Adhesion* (Dekker, New York, 1985).
21. G. C. Pimentel and A. L. McClellan, *The Hydrogen Bond* (Freeman, San Francisco, 1960).
22. Supported by grants from the Office of Naval Research (N00014-96-1-0515), NSF (DMR 93-12601), and the Department of Energy (DEFG02-91ER45439 obtained through the Materials Research Laboratory of the University of Illinois). We appreciate the efforts of P. Braun in helping with contact angle experiments, and also those of R. Strange. We acknowledge the use of facilities at the University of Illinois Center for Electron Microscopy and the Visualization Laboratory of the Beckman Institute for Advanced Science and Technology.

11 October 1996; accepted 19 February 1997